Zeitschrift für Physikalische Chemie, **215**, 12, 1601–1623 (2001)

Investigation of the Thermal Decomposition of Ketene and of the Reaction $CH_2 + H_2 \rightleftharpoons CH_3 + H$

By Gernot Friedrichs* and Heinz Gg. Wagner

Georg-August Universität Göttingen, Institut für Physikalische Chemie, Tammannstraße 6, D-37077 Göttingen, Germany

Dedicated to Prof. Dr. Dr. h.c. mult. Fritz Peter Schäfer on the occasion of his 70th birthday

(Received October 23, 2000; accepted in revised form November 6, 2000)

Chemical Kinetics / Elementary Reactions / Shock Waves / Frequency Modulation Spectroscopy / CH_2 Radicals

Using frequency modulation (FM) spectroscopy singlet methylene radicals have been detected for the first time behind shock waves. The thermal decomposition of ketene served as source for metylene radicals at temperatures from 1905 to 2780 K and pressures around 450 mbar. For the unimolecular decomposition reaction, (1) $CH_2CO + M \rightarrow CH_2 + CO + M$, the rate constants obtained are:

$$k_1 = (9.5 \pm 5.7) \cdot 10^{15} \cdot \exp\left[(-244 \pm 25)\ \mathrm{kJ\,mol^{-1}}/RT\right]\ \ \mathrm{cm^3\,mol^{-1}\,s^{-1}}.$$

As a first study of a methylene reaction at high temperatures by diretly tracing methylene the reaction of methylene with hydrogen, $(8+9)\ ^{1,3}CH_2 + H_2 \rightarrow CH_3 + H$, was investigated at temperatures from 1930 to 2455 K and pressures around 500 mbar. For the total rate constant of the singlet and triplet methylene reaction a temperature independent value was obtained:

$$\log\left(k_{8+9}/(\mathrm{cm^3\,mol^{-1}\,s^{-1}})\right) = 13.89 \pm 0.26.$$

A comparison with low temperature literature data and the systematics of activation energies of triplet methylene reactions allowed a consistent description of singlet and triplet contributions and of the forward and reverse reaction.

1. Introduction

The kinetics of the methylene radical is of interest in combustion chemistry. It is an important intermediate in hydrocarbon flames where it is mainly formed by the reaction of oxygen atoms with acetylene. Also the stepwise decomposition of higher hydrocarbon radicals can form methylene. Consecutive reaction products of methylene reactions strongly influence the product distribution

* Corresponding author. E-mail:gfriedr@gwdg.de

of the combustion process. For example, the reaction $CH_2 + O_2$ is an important chain branching reaction [1, 2] and the reaction $CH_2 + H \rightarrow CH + H_2$ is a main source for CH radicals, which may contribute to the *prompt*-NO formation via the consecutive reactions $CH + N_2 \rightarrow HCN + N$ and $N + O_2 \rightarrow NO + O$ [3]. Methylene also plays a role in forming C_3 and C_4 hydrocarbons [4].

An interesting feature of methylene reactions results from the existence of two electronic states of methylene, the triplet ground state ($^3CH_2$) and the first excited singlet state ($^1CH_2$). Since the singlet state lies only 37.6 kJ/mol [5] higher than the ground state the population of the singlet state at combustion temperatures is not negligible. At 2000 K in thermal equilibrium around 4.6% of the methylene is present as $^1CH_2$. The reactivity of both states is very different. $^3CH_2$ reacts with hydrocarbons non-stereospecific under H atom abstraction, whereas $^1CH_2$ inserts in single bonds and undergoes stereospecific addition to double bonds [6]. Normally, $^3CH_2$ reactions show rather high activation energies, while $^1CH_2$ reactions often proceed with no or very low energy barriers and the rate coefficients are comparable to the collision number. Therefore, especially at lower temperatures, the rate coefficients of the $^1CH_2$ reactions often surmount the homologous $^3CH_2$ reactions by several orders of magnitude.

Direct spectroscopic measurements of methylene reactions were performed rather extensively near ambient and elevated temperatures up to 730 K by means of Laser induced fluorescence (LIF, singlet methylene), e.g. [7–9], and Laser magnetic resonance (LMR, triplet methylene), e.g. [10–13]. However, at temperatures higher than 1000 K, which are relevant for the combustion process, studies of methylene reactions are very rare. In fact, due to low absorption coefficients and the high reactivity of methylene which results in low concentration levels of methylene, no high temperature kinetic study by directly tracing the methylene radical is found in the literature yet. Furthermore, it is just ten years ago when Sappey *et al.* [14] reported the first optical spectroscopic detection of singlet methylene at a temperature higher than 1000 K. They succeeded to detect methylene in a premixed methane/oxygen flame by means of LIF. Recently, Lozovsky *et al.* [15] and McIllroy [16] detected singlet methylene in premixed methane flames with good signal-to-noise ratios by means of Intracavity laser absorption spectroscopy (ICLAS) and Cavity ring-down spectroscopy (CRDS), respectively.

Here we report the first investigation of $^1CH_2$ reactions behind shock waves by means of frequency modulation (FM) spectroscopy which was shown to be one and a half orders of magnitude more sensitive than the normal dual beam absorption technique using narrow bandwidth laserlight [17, 18].

2. Experimental

All experiments were carried out behind incident shock waves. An aluminium shock tube with an inner diameter of 20 cm [19], equipped with a ring dye

laser (Coherent, 899–21) pumped by an Ar^+ laser (Coherent, Innova 200–15) provided a sensitive means to detect $^1CH_2$ using FM spectroscopy. The FM spectrometer used is described in detail in [18]. The electronic bandwidth of the FM spectrometer was 2.5 MHz, high enough for a time resolution of several microseconds due to the spatial extent of the laser beam. In order to adjust the laser wavelength to the $\tilde{b}\,^1B_1(0, 14, 0)4_{04} \leftarrow \tilde{a}\,^1A_1(0, 0, 0)4_{14}$ transition of $^1CH_2$ at 590.707 nm and to check the FM spectrometer settings, the laser beam passed a photolysis cell as a stationary radical source. The photolysis of gas mixtures of 5% ketene in argon at 308 nm was used to generate (quasi-) stationary $^1CH_2$ concentrations in the photolysis cell. In most experiments the laser beam passed three times through the shock tube to extend the absorption length to 60 cm. The multipassing was achieved by two small adjustable mirrors built into the shock tube wall [20]. A detection limit of approximately $2 \cdot 10^{-12}$ mol/cm^3 for $^1CH_2$ at 2200 K was achieved.

Gas mixtures of 6000 ppm ketene in argon were prepared in a stainless steel cylinder which could be evacuated to pressures lower than 10^{-7} mbar and heated up to a temperature of 500 K. A magnetic stirrer in the cylinder allowed experiments to be performed 15 min after preparation. UV absorption measurements showed that these mixtures were stable for several days. By using a flow system with calibrated mass flow controllers (Tylan, MKS) the gas mixture could be further diluted with argon or a 1% hydrogen/argon mixture, respectively. Before each experiment the shock tube was flushed with the particular mixture for about 10 min in order to reduce any influence of wall absorption.

Ketene was prepared by pyrolysis of acetone at $T = 600\,^\circ$C on Cr/Ni wires and was purified by trap to trap distillation. The purity of samples stored at 77 K was periodically checked by FTIR spectroscopy. Small impurities of ethylene ($< 2.5\%$) were found. Numerical simulations of the reaction system showed that such small amounts of ethylene did not enter critically into the evaluation. Other substances used were argon (99.998%) and hydrogen (99.999%).

For all computer simulations of the complex reaction mechanism given in Table 1 and for sensitivity analysis the Chemkin-II package [21] was used. The sensitivity coefficients σ^o were normalized with respect to the maximum concentration of the particular species over the time history. Except for CH_2, which will be discussed in the next section, all thermochemical data were taken from Konnov [22].

3. Evaluation

For the decomposition of ketene the following channels may be considered:

$$\text{(1a)} \quad CH_2CO + M \rightleftharpoons {}^3CH_2 + CO + M \qquad \Delta_r H^\circ_{298K} = 328\,\text{kJ/mol}$$

$$\text{(1b)} \quad \rightleftharpoons {}^1CH_2 + CO + M \qquad 366\,\text{kJ/mol}$$

(1c)	$\rightleftharpoons C_2O + H_2 + M$	433 kJ/mol
(1d)	$\rightleftharpoons HCCO + H + M$	443 kJ/mol
(1e)	$\rightleftharpoons C_2H + OH + M$	634 kJ/mol
(1f)	$\rightleftharpoons C_2 + H_2O + M$	637 kJ/mol
(1g)	$\rightleftharpoons HCO + CH + M$	687 kJ/mol.

Because of the high endothermicity the three channels (1e)–(1g) should not contribute to the decomposition, whereas the other channels might get some influence especially at high temperatures. Channel (1b) yields singlet methylene which is rapidly quenched under the experimental conditions applied:

$$(2) \qquad {}^1CH_2 + M \rightleftharpoons {}^3CH_2 + M \qquad \Delta_r H^\circ_{298\,K} = -37.6\,\text{kJ/mol}.$$

Carstensen [23] determined the quenching rate of ${}^1CH_2$ by argon at temperatures from 206 to 547 K. Using his expression for k_2, $2.41 \cdot 10^{10} \cdot T^{0.9}$, and assuming an average total density of $2.5 \cdot 10^{-6}$ mol/cm^3 the thermal equilibrium should be reached within 250 ns which is much faster than the time resolution of the shock tube apparatus (7 μs). As a result of the thermal equilibrium between singlet and triplet methylene on the one hand the experimental ${}^1CH_2$ concentration time profiles could be taken as a measure for the total methylene concentration in the reaction system. On the other hand it was not possible to distinguish between singlet and triplet reactions in general and between channel (1a) and (1b) in particular.

Channel (1c) would yield C_2O which decomposes fast to C atoms and CO [24]. Markus *et al.* [25] investigated the thermal decomposition of ketene by means of C-Atomic resonance absorption spectroscopy (C-ARAS) and ruled out channel (1c) to be a direct decomposition channel. Frank *et al.* [26] also investigated the thermal decomposition of ketene at temperatures from 1650 to 2800 K by means of resonant detection of H atoms and CO. At temperatures from 2000 to 2300 K channel (1d) was found to show a 10% contribution. At higher temperatures a possible influence of channel (1b) on the measured H atom profiles could not be distinguished from other H atom forming secondary reactions. Bauerle *et al.* [27] inferred channel (1d) to be less significant ($< 5\%$) from their H atom measurements up to temperatures of 2700 K.

For a quantitative evaluation of the singlet methylene profiles the equilibrium constant and with it the energy difference between singlet and triplet methylene (singlet triplet splitting Δ_{ST}) had to be known accurately [5, 28–30]. In this work $\Delta_{ST} = 3147\,\text{cm}^{-1} \mathrel{\hat{=}} 37.6\,\text{kJ/mol}$ was used which is in good agreement with the data of [5] and [30]. For the enthalpies of formation of methylene values of $\Delta_f H^\circ_{298\,K}({}^3CH_2) = 391.0\,\text{kJ/mol}$ [31, 32] and $\Delta_f H^\circ_{298\,K}({}^1CH_2) = 428.6\,\text{kJ/mol}$ were used. The temperature dependence of the enthalpies and entropies of formation were taken from the thermodynamic

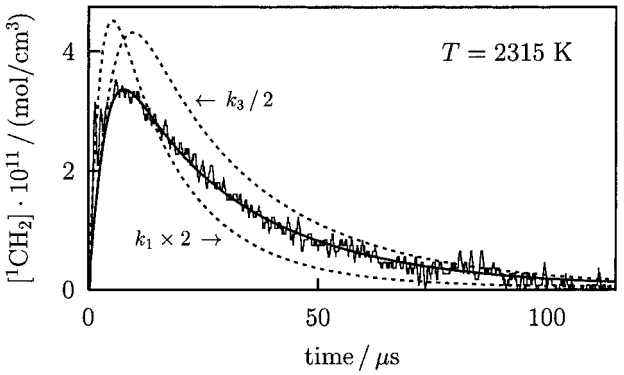

Fig. 1. Experimental and simulated $^1CH_2$ concentration profiles. $T = 2315$ K, $\varrho = 2.58 \cdot 10^{-6}$ mol/cm^3, 1195 ppm ketene; solid lines: experiment and best fit; dashed lines: simulations with $k_1 \times 2$ and $k_3/2$; (1) $CH_2CO + M \rightleftharpoons CH_2 + CO + M$ and (3a + 3b) $CH_2 + CH_2 \rightleftharpoons C_2H_2 + 2H$ resp. $C_2H_2 + H_2$. The maximum of the $^1CH_2$ concentration profile corresponds to 13 ppm $^1CH_2$.

database of GRI-Mech 3.0 [33]. Using these values equilibrium constants for reaction (2) of $K = 23.2$, 14.9, 11.0 and hence singlet methylene fractions ($[^1CH_2]/[CH_2]_{tot}$) of 4.1%, 6.3%, 8.4% at 1900, 2350 and 2800 K were obtained, respectively.

The thermal decomposition of ketene was investigated behind incident shock waves in the temperature range from 1905 to 2780 K and densities ranging from 1.6 to $3.4 \cdot 10^{-6}$ mol/cm^3 which correspond to pressures of 370 – 530 mbar. Most experiments were performed by multipassing the detection laser three times through the shock tube (3×20 cm). Control experiments with a single path of the laser beam were performed. These experiments provided consistent results. The initial mole fraction of ketene varied from 395 – 2605 ppm (multipass) and 1200 – 5400 ppm (single pass), respectively.

In Fig. 1 an experiment at a temperature of 2315 K, a total density of $2.58 \cdot 10^{-6}$ mol/cm^3 and an initial ketene mole fraction of 1195 ppm is shown. The $^1CH_2$ concentration reaches its maximum value after 7–8 μs and is near zero again after 100 μs. The initial increase is determined by the unimolecular decomposition of ketene (reaction (1)). For the evaluation it was assumed to proceed via channel (1a) yielding quantitatively $^3CH_2$ which rapidly equilibrates with $^1CH_2$.

The following decrease of CH_2 is due to fast consecutive reactions of methylene with itself, with ketene and with other species, e.g.

(3) $CH_2 + CH_2 \rightarrow$ products

(3a) $CH_2 + CH_2 \rightleftharpoons C_2H_2 + H + H \quad \Delta_r H^\circ_{298\,K} = -119$ kJ/mol

(3b) $\rightleftharpoons C_2H_2 + H_2 \quad -555$ kJ/mol.

Here and within the following text CH_2 is used instead of $^3CH_2$ and $^1CH_2$ in cases where no seperate literature data are available. For numerical analysis in these cases CH_2 was set equal to $^3CH_2$. That should be a good approximation since $^3CH_2$ is the excess species (see above).

Frank *et al.* [26] concluded that from 2100 to 2700 K reaction (3) proceeds via channel (3a) yielding two H atoms with a rate constant of $1 \cdot 10^{14}$ $cm^3\,mol^{-1}\,s^{-1}$. Such a quantitative H atom yield is in disagreement with measurement of Dombrowsky *et al.* [2] who investigated the reaction $CH_2 + O_2 \rightarrow$ products by tracing OH radicals. Assuming a quantitative H atom yield of the side reaction (3) would have resulted in a much higher OH concentration and faster OH formation via the reaction $H + O_2 \rightarrow O + OH$ than measured. Bauerle *et al.* [27] also investigated the thermal decomposition of ketene and diazomethane behind shock waves by means of H-ARAS and concluded that channel (3a) contributes 10–20% to the total reaction (3) at temperatures from 1100 to 2700 K. They reported a total rate constant of $1.3 \cdot 10^{14}$ $cm^3\,mol^{-1}\,s^{-1}$ at 2300 K which is in good agreement with the rate constant reported by Frank *et al.*

Other channels like

$$\begin{aligned}
&\text{(3c)} \quad CH_2 + CH_2 \rightleftharpoons C_2H_4 && \Delta_r H^\circ_{298\,K} = -730\,kJ/mol\\
&\text{(3d)} \quad \rightleftharpoons C_2H_3 + H && -264\,kJ/mol\\
&\text{(3e)} \quad \rightleftharpoons CH + CH_3 && -38\,kJ/mol,
\end{aligned}$$

are of minor importance for the experimental conditions used here. C_2H_3 which would be formed via channel (3d) decomposes fast yielding C_2H_2 and H. Thus, channel (3d) is indistinguishable from channel (3a). The formation of CH_3 via channel (3e), as proposed by Frank and Just [34], could not be verified by Dombrowsky [35] during the thermal decomposition of diazomethane at temperatures from 900 to 1400 K. Markus *et al.* [25] measured CH radical profiles during the thermal decomposition of ketene at temperatures from 2200 to 3400 K and they concluded that approximately 6% of reaction (3) proceed via channel (3e).

Next to reaction (3) the reactions of methylene with ketene and the reaction of methylene with H atoms shall be considered.

For the reactions

$$\begin{aligned}
&\text{(4)} \quad {}^3CH_2 + H \rightleftharpoons CH + H_2 && \Delta_r H^\circ_{298\,K} = -12\,kJ/mol\\
&\text{(5)} \quad {}^1CH_2 + H \rightleftharpoons CH + H_2 && \Delta_r H^\circ_{298\,K} = -50\,kJ/mol
\end{aligned}$$

several investigations are reported in the literature. For reaction (4) we refer to the publication of Hippler *et al.* [36] who recently compared their new experimental results with literature data and SACM calculations. We used a temperature independent value of $k_4 = 1.1 \cdot 10^{14}$ $cm^3\,mol^{-1}\,s^{-1}$. In addition, reaction (5) was taken into account with $k_5 = 7 \cdot 10^{13}$ $cm^3\,mol^{-1}\,s^{-1}$ based on an estimation of Peeters *et al.* [37].

There are some bimolecular reactions of ketene which might have some influence especially at lower temperatures, e.g.

(6a)	$^3CH_2 + CH_2CO \rightleftharpoons C_2H_4 + CO$	$\Delta_r H^\circ_{298\,K} = -401\,kJ/mol$
(6b)	$^3CH_2 + CH_2CO \rightleftharpoons CH_3 + HCCO$	$-19\,kJ/mol$
(7a)	$^1CH_2 + CH_2CO \rightleftharpoons C_2H_4 + CO$	$-439\,kJ/mol$
(7b)	$^1CH_2 + CH_2CO \rightleftharpoons CH_3 + HCCO$	$-57\,kJ/mol.$

Carstensen [23] determined the rate of the reaction $^1CH_2 + CH_2CO \rightarrow$ products at temperatures from 240 to 510 K to be $(1.5 \pm 0.2) \cdot 10^{14} \cdot (T/293\,K)^{-0.45\pm0.45}$ $cm^3\,mol^{-1}\,s^{-1}$. This rate constant represents the sum of the quenching process ($\rightarrow {}^3CH_2 + CH_2CO$) and the reactive process. Thus, this expression, which has been used here for the evaluation, gives an upper limit for this rate. On the basis of the quantum yield of CO and C_2H_4 following the photodissociation of CH_2CO ($\phi_{CO}/\phi_{C_2H_4} = 2.2$ [38]) Böhland *et al.* [11] concluded that the quenching process should be of minor importance. The reaction of triplet methylene with ketene should be relatively slow. Based on estimations of this reaction in [26, 27], k_6 was estimated to be $1 \cdot 10^{12}$ $cm^3\,mol^{-1}\,s^{-1}$. In thermal equilibrium at 2000 K (4.6% $^1CH_2$) approximately 75% of the total methylene consumption by reaction (6) and (7) is due to the singlet reaction (7). The individual product channels (a) and (b) are assumed to contribute equally to the total rate constants of reactions (6) and (7).

Next to the reactions just mentioned several other reactions can influence the measured $^1CH_2$ concentration profiles. In Table 1 the mechanism used for the simulations is given.

It is devided into five groups. Reactions (1) and (2) represent the start reactions, reactions (3)–(16) take into account bimolecular reactions of both singlet and triplet methylene, reactions (17) and (18) specify reactions of ketene with H and H_2, reactions (19)–(27) summarize bimolecular reactions of other reactive species and finally reactions (28)–(39) list unimolecular decomposition reactions of the intermediate species.

In some cases singlet ($^1CH_2$) and triplet ($^3CH_2 \mathrel{\hat{=}} CH_2$) reactions are taken into account seperately. In all other cases the triplet reactions hold for the sum of singlet *and* triplet reaction.

For a first evaluation of the experimental $^1CH_2$ profiles only the rate constant of reaction (1) and a scaling factor, which converts the measured signal level to $^1CH_2$ concentration, were used as free parameters. The scaling was needed because the absorption coefficient of $^1CH_2$ was unknown. In Fig. 1 the influence of reaction (1) on the simulated profile is shown. Next to the solid line (best fit) a simulation with $k_1 \times 2$ is shown, which results in a maximum $^1CH_2$ concentration at a shorter reaction time and a subsequent faster decrease. Scaling the signal to this *new* maximum would have resulted in a worse fit. Thus, with all other rate coefficients held constant, a reliable determination of k_1 and the scaling factor was possible.

Table 1. Reaction mechanism: Rate constants are given in $k_i = A \cdot T^n \cdot \exp(E_a/RT)$ (units kJ, cm^3, mol, s and K). CH_2 is equal to $^3CH_2$.

No.	Reaction	A	n	E_a	Ref.
	Start Reactions				
1	$CH_2CO + M \rightleftharpoons CH_2 + CO + M$	$9.5 \cdot 10^{15}$	0	244	**
2	$^1CH_2 + M \rightleftharpoons CH_2 + M$	$2.4 \cdot 10^{10}$	0.9	0	[23]
	Reactions $CH_2 + X$ and $^1CH_2 + X$				
3a	$CH_2 + CH_2 \rightleftharpoons C_2H_2 + H + H$	$3.8 \cdot 10^{14}$	0	29.5	**
3b	$CH_2 + CH_2 \rightleftharpoons C_2H_2 + H_2$	$3.8 \cdot 10^{14}$	0	29.5	**
4	$CH_2 + H \rightleftharpoons CH + H_2$	$1.1 \cdot 10^{14}$	0	0	[36, 39]
5	$^1CH_2 + H \rightleftharpoons CH + H_2$	$7.0 \cdot 10^{13}$	0	0	[37], est.
6a	$CH_2 + CH_2CO \rightleftharpoons C_2H_4 + CO$	$5.0 \cdot 10^{11}$	0	0	est.
6b	$CH_2 + CH_2CO \rightleftharpoons CH_3 + HCCO$	$5.0 \cdot 10^{11}$	0	0	est.
7a	$^1CH_2 + CH_2CO \rightleftharpoons C_2H_4 + CO$	$9.5 \cdot 10^{14}$	−0.45	0	[23]***
7b	$^1CH_2 + CH_2CO \rightleftharpoons CH_3 + HCCO$	$9.5 \cdot 10^{14}$	−0.45	0	[23]***
8	$CH_2 + H_2 \rightleftharpoons CH_3 + H$	$1.0 \cdot 10^{13}$	0	51	**, ****
9	$^1CH_2 + H_2 \rightleftharpoons CH_3 + H$	$6.8 \cdot 10^{13}$	0	0	**, ****
10a	$CH_2 + C_2H_2 \rightleftharpoons C_3H_3 + H$	$6.0 \cdot 10^{12}$	0	28	[40]***
10b	$CH_2 + C_2H_2 \rightarrow AC_3H_4*$	$6.0 \cdot 10^{12}$	0	28	[40]***
11a	$^1CH_2 + C_2H_2 \rightleftharpoons C_3H_3 + H$	$1.1 \cdot 10^{14}$	0	0	[40]***
11b	$^1CH_2 + C_2H_2 \rightarrow AC_3H_4*$	$1.1 \cdot 10^{14}$	0	0	[40]***
12	$CH_2 + CH \rightleftharpoons C_2H_2 + H$	$1.0 \cdot 10^{14}$	0	0	[27], est.
13	$CH_2 + C_2H_4 \rightleftharpoons C_3H_6$	$3.2 \cdot 10^{12}$	0	22	[41]
14	$^1CH_2 + C_2H_4 \rightleftharpoons C_3H_6$	$1.1 \cdot 10^{14}$	0	0	[8]
15	$CH_2 + CH_3 \rightleftharpoons C_2H_4 + H$	$4.2 \cdot 10^{13}$	0	0	[40]
16	$^1CH_2 + CH_3 \rightleftharpoons C_2H_4 + H$	$1.8 \cdot 10^{13}$	0	0	[42]
	Suppl. Ketene Reactions				
17a	$H + CH_2CO \rightleftharpoons CH_3 + CO$	$1.8 \cdot 10^{13}$	0	14	[40]
17b	$H + CH_2CO \rightleftharpoons HCCO + H_2$	$5.0 \cdot 10^{13}$	0	33	[43]
18a	$H + CH_3CO \rightleftharpoons CH_2CO + H_2$	$3.3 \cdot 10^{13}$	0	0	[44]
18b	$H + CH_2HCO \rightleftharpoons CH_2CO + H_2$	$2.0 \cdot 10^{13}$	0	0	[45]
18c	$O + C_2H_4 \rightleftharpoons CH_2CO + H_2$	$6.7 \cdot 10^{5}$	1.88	0.8	[46]
	Suppl. Bimolecular Reactions				
19	$H + C_2H_2 \rightleftharpoons H_2 + C_2H$	$6.0 \cdot 10^{13}$	0	116	[40]
20	$H + C_2H_4 \rightleftharpoons H_2 + C_2H_3$	$5.4 \cdot 10^{14}$	0	62	[40]
21	$CH + C_2H_2 \rightleftharpoons H + C_3H_2$	$1.3 \cdot 10^{14}$	0	0	[47]
22	$HCCO + C_2H_2 \rightleftharpoons C_3H_3 + CO$	$1.0 \cdot 10^{11}$	0	13	[4, 48]
23	$HCCO + HCCO \rightleftharpoons C_2H_2 + CO + CO$	$1.0 \cdot 10^{13}$	0	0	[4]
24	$CH + CH \rightleftharpoons C_2H + H$	$1.5 \cdot 10^{14}$	0	0	[49]
25	$CH_3 + CH_3 \rightarrow C_2H_5 + H$	$3.0 \cdot 10^{13}$	0	57	[40]
26	$H + C_2H_5 \rightleftharpoons C_2H_4 + H$	$2.0 \cdot 10^{12}$	0	0	[40]
27	$CH_3 + H_2 \rightleftharpoons CH_4 + H$	$2.0 \cdot 10^{13}$	0	60	[51]

continued on the next page →

However, using the rate expressions for the important reactions (3a) and (3b) given in [27] for the first evaluation, rate constants k_1 were obtained which showed an unexpected but obvious deviation from a linear Arrhenius be-

Table 1. continued.

No.	Reaction	A	n	E_a	Ref.
Suppl. Unimolecular Decompositions					
28	$CH + M \rightarrow C + H + M$	$1.9 \cdot 10^{14}$	0	280	[50]
29a	$CH_2 + M \rightarrow C + H_2 + M$	$1.6 \cdot 10^{14}$	0	268	[25]
29b	$CH_2 + M \rightleftharpoons CH + H + M$	$5.6 \cdot 10^{15}$	0	375	[27]
30a	$CH_3 + M \rightleftharpoons {}^1CH_2 + H + M$	$1.9 \cdot 10^{16}$	0	383	[52]
30b	$CH_3 + M \rightleftharpoons CH + H_2 + M$	$4.2 \cdot 10^{15}$	0	345	[53]
31	$CH_4 + M \rightleftharpoons CH_3 + H + M$	$2.0 \cdot 10^{17}$	0	368	[54]
32	$C_2H + M \rightarrow C_2 + H + M$	$8.0 \cdot 10^{14}$	0	342	[55]
33	$C_2H_2 + M \rightleftharpoons C_2H + H + M$	$4.0 \cdot 10^{16}$	0	447	[56]
34	$C_2H_3 + M \rightleftharpoons C_2H_2 + H + M$	$4.2 \cdot 10^{41}$	−7.5	190	[40]
35a	$C_2H_4 + M \rightleftharpoons C_2H_2 + H_2 + M$	$2.6 \cdot 10^{17}$	0	332	[56]
35b	$C_2H_4 + M \rightleftharpoons C_2H_3 + H + M$	$2.6 \cdot 10^{17}$	0	404	[56]
36	$C_3H_3 + M \rightleftharpoons C_3H_2 + H + M$	$2.0 \cdot 10^{48}$	−8.5	410	[57], est.
37	$C_3H_6 \rightleftharpoons C_2H_3 + CH_3$	$1.1 \cdot 10^{21}$	−1.2	409	[58]
38	$HCCO + M \rightleftharpoons CH + CO + M$	$6.0 \cdot 10^{15}$	0	246	[59]
39	$H_2 + M \rightleftharpoons H + H + M$	$6.0 \cdot 10^{18}$	−1.1	437	[60]

* Allen ($H_2C = C = CH_2$).
** this work.
*** channel distribution estimated.
**** $k_{8+9} = 7.8 \cdot 10^{13}$ $cm^3\,mol^{-1}\,s^{-1}$.
est.: estimated.

havior at lower temperatures. Furthermore, the absorption coefficient, which could be calculated from the obtained scaling factors, showed a pronounced maximum at a temperature around 2200 K whereas a simple population analysis predicts a uniform increase of the absorption coefficient with decreasing temperature at the experimental conditions used. Both effects clearly indicate that, at low temperatures in particular, bimolecular reactions have a more pronounced influence on the profiles than predicted from the mechanism used for this first evaluation.

In Fig. 2 two experiments at a temperature of 1965 K and 2535 K are shown, respectively. For sensitivity analysis, which is shown in the upper and lower part of Fig. 2, only the most sensitive reactions are shown. At both temperatures the reactions (1) and (3) are the dominant reactions, but also reaction (4) has a noticeable influence, whereas reaction (7) is important only at low temperatures. The high sensitivity coefficients of reaction (3a) and (3b) suggest these reactions to be responsible for the observed deviations in k_1 and the absorption coefficient. It was found in a second evaluation that the following rate expressions for reaction (3a) and (3b) allow a good description of the experimental methylene profiles and, beyond it, result in consistent data for k_1 and the absorption coefficient:

$$k_{3a} = k_{3b} = 3.8 \cdot 10^{14} \cdot \exp\left(-29.5\,\mathrm{kJ/mol}/\,RT\right)\ \mathrm{cm^3\,mol^{-1}\,s^{-1}}.$$

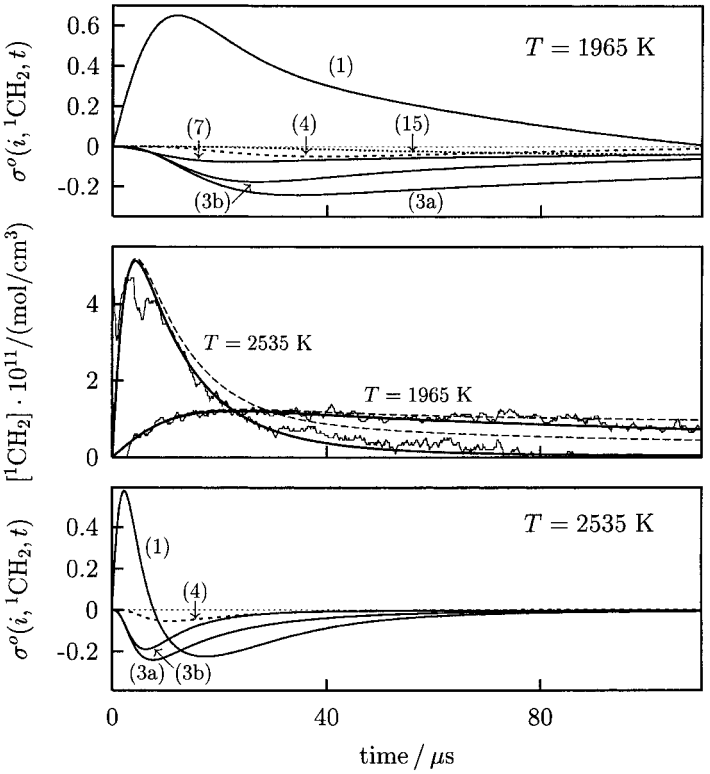

Fig. 2. $^1CH_2$ concentration profiles and sensitivity analysis for two experiments. $T = 1965$ K, $\varrho = 3.22 \cdot 10^{-6}$ mol/cm^3, 1500 ppm ketene and $T = 2535$ K, $\varrho = 1.87 \cdot 10^{-6}$ mol/cm^3, 1245 ppm ketene. Middle: experimental $^1CH_2$ profils and best fits (solid lines). The dashed lines refer to simulations using a reduced mechanism (reactions (1–4) and (7)). Upper and lower: sensitivity analysis. (1) $CH_2CO + M \rightleftharpoons CH_2 + CO + M$, (2) $^1CH_2 + M \rightleftharpoons {}^3CH_2 + M$, (3a) $2\,CH_2 \rightleftharpoons C_2H_2 + 2\,H$, (3b) $2\,CH_2 \rightleftharpoons C_2H_2 + H_2$, (4) $^3CH_2 + H \rightleftharpoons CH + H_2$, (7a + 7b) $^1CH_2 + CH_2CO \rightleftharpoons$ products, (15) $^3CH_2 + CH_3 \rightleftharpoons C_2H_4 + H$.

Compared to the rate constants of Bauerle *et al.* [27] this expression gives a 1.5 times larger rate constant k_3 at 1900 K, but the same value at 2800 K. The channel distribution is changed from 10–20% in [27] to 50%. The resulting higher H atom yield also increases the importance of reaction (4) ($^3CH_2 + H$).

It should be mentioned here that higher values of k_3 without changing the channel distribution did not result in consistent data. However, an increase of the rates of reactions (4), (7) or choosing a higher rate for ketene decomposition channel (1d) result in a tendency of the evaluated data quite similar to the performed change of k_{3a} and k_{3b}. As expected from the sensitivity analysis shown in Fig. 2 these variations would however have been more pronounced than the changes introduced here. Overall, H atom yields

Table 2. Experimental conditions and results: Unimolecular decomposition of ketene and $^1CH_2$ calibration function ζ (scaling factor).

No.	T / K	$10^6 \cdot \varrho$ [mol cm^{-3}]	$x(CH_2CO)$ [ppm]	k_1 [cm^3 mol^{-1} s^{-1}]	$10^{-8} \cdot \zeta(T)$ [cm^3/mol]
$l = 20$ cm, single pass	($\zeta(T)$ is adjusted to $l = 60$ cm)				
k24	2085	2.78	5400	$7.5 \cdot 10^9$	2.97
k23	2090	2.79	3240	$7.0 \cdot 10^9$	2.25
k27	2135	2.80	3090	$5.5 \cdot 10^9$	2.09
k33	2145	2.80	3090	$6.0 \cdot 10^9$	2.36
k25	2280	2.75	3090	$1.7 \cdot 10^{10}$	2.04
k45	2290	2.55	1200	$2.4 \cdot 10^{10}$	2.25
k44	2315	2.55	2600	$2.7 \cdot 10^{10}$	2.47
k37	2350	2.28	2800	$2.8 \cdot 10^{10}$	1.89
k20	2400	2.28	1680	$5.5 \cdot 10^{10}$	1.95
k19	2430	2.28	5400	$6.0 \cdot 10^{10}$	1.73
l=60 cm, multipass					
k72	1905	3.35	1000	$1.6 \cdot 10^9$	2.83
k93	1940	3.45	1115	$4.5 \cdot 10^9$	2.45
k74	1965	3.22	1500	$1.9 \cdot 10^9$	2.47
k91	1975	3.44	1045	$5.0 \cdot 10^9$	2.67
k83	1990	3.06	1245	$4.5 \cdot 10^9$	2.38
k98	1995	3.34	1500	$5.0 \cdot 10^9$	2.74
k89	2030	3.03	975	$8.0 \cdot 10^9$	2.76
k70	2060	2.82	1000	$8.0 \cdot 10^9$	2.90
k71	2065	3.11	1000	$6.7 \cdot 10^9$	2.47
k99	2085	2.88	2605	$9.0 \cdot 10^9$	2.25
k77	2125	3.04	1000	$6.5 \cdot 10^9$	2.11
k92	2175	2.54	1045	$1.8 \cdot 10^{10}$	2.54
k64	2185	2.58	955	$1.4 \cdot 10^{10}$	2.61
k61	2185	2.59	950	$1.7 \cdot 10^{10}$	2.25
k60	2195	2.56	950	$1.6 \cdot 10^{10}$	2.54
k97	2255	2.56	1500	$2.3 \cdot 10^{10}$	2.11
k84	2280	2.20	1245	$2.6 \cdot 10^{10}$	1.91
k94	2300	2.55	1115	$2.6 \cdot 10^{10}$	2.38
k52	2315	2.58	1195	$2.1 \cdot 10^{10}$	(3.41)
k81	2330	2.56	1245	$2.4 \cdot 10^{10}$	1.89
k87	2365	2.36	1215	$3.2 \cdot 10^{10}$	2.00
k95	2415	2.29	1115	$4.3 \cdot 10^{10}$	1.59
k56	2460	1.94	1195	$8.0 \cdot 10^{10}$	1.80
k58	2485	1.94	395	$9.0 \cdot 10^{10}$	1.73
k57	2500	1.92	1195	$1.1 \cdot 10^{11}$	1.95
k85	2535	1.87	1245	$8.5 \cdot 10^{10}$	1.46
k88	2620	1.88	730	$1.6 \cdot 10^{11}$	1.37
k86	2640	1.88	750	$1.1 \cdot 10^{11}$	1.24
k80	2780	1.61	1000	$2.5 \cdot 10^{11}$	1.12

higher than those reported by Bauerle *et al.* seem very probable. The experimental conditions, obtained values for k_1 and the scaling factors are listed in Table 2.

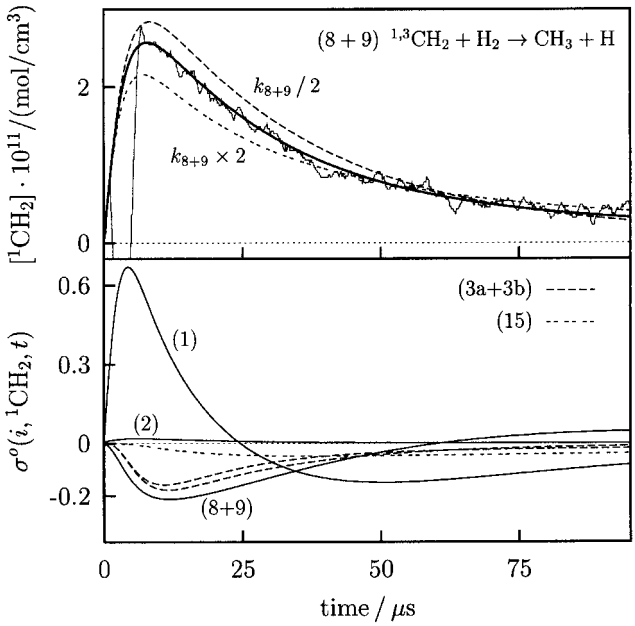

Fig. 3. Experimental profile and sensitivity analysis. $T = 2210$ K, $\varrho = 2.41 \cdot 10^{-6}$ mol/cm^3, 1550 ppm ketene, 6120 ppm hydrogen, $[H_2]_o : [CH_2CO]_o = 4 : 1$. Upper: solid lines – experiment and best fit; dashed lines – simulations with $k_{8+9} \times 2$ and $k_{8+9}/2$. Lower: sensitivity analysis of same experiment; (1) $CH_2CO + M \rightleftharpoons CH_2 + CO + M$, (2) $^1CH_2 + M \rightleftharpoons {}^3CH_2 + M$, (3a) $CH_2 + CH_2 \rightleftharpoons C_2H_2 + H + H$, (3b) $CH_2 + CH_2 \rightleftharpoons C_2H_2 + H_2$, (8+9) $^{1,3}CH_2 + H_2 \rightarrow CH_3 + H$, (15) $^3CH_2 + CH_3 \rightleftharpoons C_2H_4 + H$.

Having once established the ketene decomposition mechanism, H_2 was added to the intitial gas mixture to increase the influence of the reaction of methylene with hydrogen:

(8) $^3CH_2 + H_2 \rightleftharpoons CH_3 + H$ $\quad \Delta_r H^\circ_{298\,K} = -26.0$ kJ/mol
(9) $^1CH_2 + H_2 \rightleftharpoons CH_3 + H$ $\quad -63.6$ kJ/mol.

Experiments were performed behind incident shock waves in the temperature range 1930–2455 K and densities ranging from 2.3 to $3.2 \cdot 10^{-6}$ mol/cm^3 which correspond to pressures of 458 to 515 mbar. Initial mixtures of 1115–1495 ppm ketene in argon served as methylene source. The mole fraction of H_2 was chosen to be 6360–14 450 ppm, thus a factor of 4 – 10 higher than ketene.

In the upper part of Fig. 3 an experiment at a temperature of 2210 K and a hydrogen excess of 4 is shown. The partly negative signal during the first 6 μs is due to the passage of the shock wave through the detection plane of the laser beam (Schlieren signal). The thick solid line was obtained by numerical

simulation of the reaction system. As $^1CH_2$ and $^3CH_2$ were not distinguishable, reaction (8) was neglected and reaction (9) was used as an adjustable parameter. Therefore the obtained rate constant represents the total rate constant k_{8+9}. The scaling factor was varied within its error limits.

The influence of the reaction $(8+9)$ on the $^1CH_2$ profile is illustrated in Fig. 3. In the upper part two simulations are shown with k_{8+9} chosen twice and half of the best fit value. In the lower part the sensitivity analysis reveals that reaction $(8+9)$ has become as sensitive as reactions (3a) or (3b). Thus a reliable determination of this rate constant should be possible. Due to the methyl radicals formed via reation $(8+9)$ at longer reaction times reaction (15), $^3CH_2 + CH_3 \rightleftharpoons C_2H_4 + H$, becomes important. Furthermore, at these long reaction times the sensitivity coefficient of reaction $(8+9)$ changes its sign from negative to positive values. This could be interpreted in a way that reaction $(8+9)$ becomes a methylene source, thus mainly taking place in the reverse direction due to a strong H formation via several consecutive reactions. In contrast to the pure ketene decomposition reaction (2), $^1CH_2 + M \rightleftharpoons {}^3CH_2 + M$, shows little influence on the detected profiles. Due to the fast reaction of $^1CH_2$ with hydrogen the thermal equilibrium of singlet and triplet methylene is not fully established. However, in the example given in Fig. 3 $^1CH_2$ still reaches at least 96% of its equilibrium concentration. Such small deviations were negligible for the evaluation.

Next to the experimental conditions the obtained values for k_{8+9} are listed in Table 3.

4. Results and discussion

Reaction (1)

The obtained values for the rate constant of the unimolecular decomposition of ketene

$$(1) \quad CH_2CO + M \rightarrow {}^3CH_2 + CO + M \qquad \Delta_r H^\circ_{298\,K} = 328\,\mathrm{kJ/mol}$$

are plotted as function of temperature (filled circles) and are compared to other literature values in Fig. 4. At temperatures from 1905 to 2780 K and densities from 1.6 to $3.4 \cdot 10^{-6}$ mol/cm^3 they can be represented by the expression (thick solid line):

$$k_1 = (9.5 \pm 5.7) \cdot 10^{15} \cdot \exp\left[(-244 \pm 25)\ \mathrm{kJ\,mol^{-1}} \,/\, RT\right] \quad \mathrm{cm^3\,mol^{-1}\,s^{-1}}.$$

Wagner and Zabel [61] investigated the thermal decomposition of ketene at temperatures from 1300 to 2000 K at total densities from $5.0 \cdot 10^{-5}$ to $2 \cdot 10^{-3}$ mol/cm^3 behind reflected shock waves. Ketene profiles were measured by means of UV absorption at 220 and 230 nm. As expected for a five-atom molecule the unimolecular decomposition took place in the *fall-off*

Table 3. Experimental conditions and results: (8 + 9) $CH_2 + H_2 \rightleftharpoons CH_3 + H$.

No.	T / K	$10^6 \cdot \varrho$ [mol cm^{-3}]	$x(CH_2CO)$ [ppm]	$x(H_2)$ [ppm]	$\frac{[H_2]_o}{[CH_2CO]_o}$	$k_{8+9} \cdot 10^{-13}$ [cm^3 mol^{-1} s^{-1}]
kh01	2160	2.54	1115	6360	5.7	7
kh04	2310	2.56	1115	6360	5.7	7
kh05	2455	2.31	1115	6360	5.7	11
kh06	2395	2.30	1115	6360	5.7	12
kh07	2125	2.84	1115	6360	5.7	12
kh10	1930	3.21	1115	6360	5.7	5
kh11	2110	3.06	1115	6360	5.7	10
kh13	1990	3.07	1550	6130	4.0	8
kh14	2210	2.41	1550	6130	4.0	8
kh15	2185	2.56	1285	10850	8.4	6
kh16	2020	2.81	1285	10850	8.4	7
kh17	2110	2.55	1495	14450	9.7	5

region. For a total density of $6 \cdot 10^{-5}$ mol/cm^3, the low density range of their experiments, they reported an Arrhenius expression of $k_1 = 3.6 \cdot 10^{15} \cdot \exp(-247\,\text{kJ mol}^{-1}/RT)$ cm^3 mol^{-1} s^{-1} which is shown in Fig. 4 as solid line marked with open triangles. Frank *et al.* [26] investigated the thermal decomposition of ketene behind shock waves by means of Molecular resonance absorption spectroscopy (MolRAS) of carbon monoxide. For temperatures of 1650 to 1850 K and an average total density of $1.2 \cdot 10^{-5}$ mol/cm^3 they obtained $k_1 = 2.3 \cdot 10^{15} \cdot \exp(-241\,\text{kJ mol}^{-1}/RT)$ cm^3 mol^{-1} s^{-1} (open squares) which is in very good agreement with the expression given in [61]. An extrapolation of the expressions of Frank *et al.* and Wagner and Zabel towards higher temperatures would result in lower values for k_1 than measured in this work. Since our expression is obtained at 5–25 times lower total densities ($\varrho \sim 2.5 \cdot 10^{-6}$ mol/cm^3) this is an indication, that the rate of the thermal decomposition of ketene has not yet reached its low pressure limit value at densities of $6 \cdot 10^{-5}$ mol/cm^3 used in [61]. Generally, a second order evaluation of a unimolecular reaction, which takes place in the fall off region, yields too low second order rate constants.

In the GRI-Mechanism [33] the rate k_{-1} of the recombination reaction (-1) is given as a function of temperature and pressure. The reported expression is based on a RRKM calculation assuming a recombination barrier of 18.8 kJ/mol. The calculation was fitted to reproduce the experimental values of Wagner and Zabel and Frank *et al.* In Fig. 4 the corresponding values for an average total density of $6 \cdot 10^{-5}$ mol/cm^3 (dashed line marked with crosses) and $2.5 \cdot 10^{-6}$ mol/cm^3 (dashed line marked with stars) are shown, respectively. The GRI-Mech data result in merely 30% lower values than measured in this work.

As the GRI-Mech data were also fitted to the high pressure experimental values of [61] (not shown in Fig. 4), they are in good agreement with all ex-

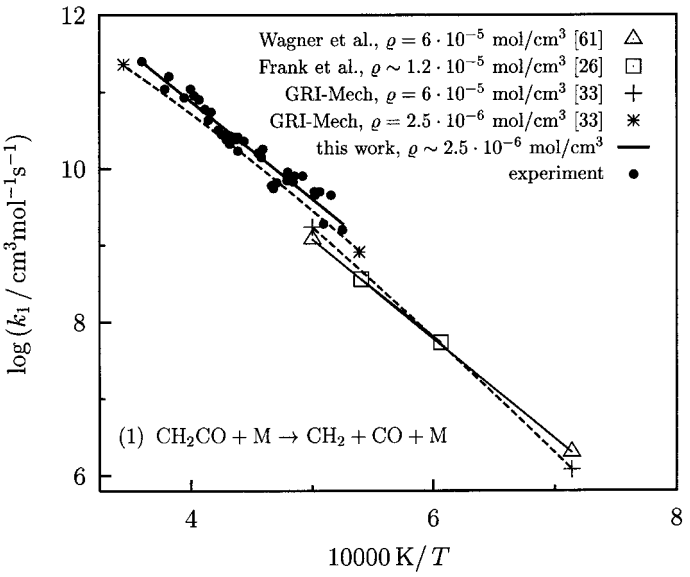

Fig. 4. Arrhenius plot of reaction (1) $CH_2CO + M \rightarrow CH_2 + CO + M$.

perimental data over a wide range of temperatures (1300–2780 K) and total densities ($1.6 \cdot 10^{-6} - 2 \cdot 10^{-3}$ mol/cm^3). The assumed recombination barrier of 18.8 kJ/mol might be somewhat too high. Recently published results are from Kim *et al.* (15.3 kJ/mol, experimental value [62]) and from King *et al.* (17.8 kJ/mol, theoretical value [63]).

Reaction (8+9)

The obtained values for the total rate constant k_{8+9} of the reaction of methylene with hydrogen

$$\begin{aligned} &(8) \quad {}^3CH_2 + H_2 \rightarrow CH_3 + H \qquad \Delta_r H^\circ_{298\,\mathrm{K}} = -26.0\,\mathrm{kJ/mol} \\ &(9) \quad {}^1CH_2 + H_2 \rightarrow CH_3 + H \qquad\qquad\quad -63.6\,\mathrm{kJ/mol} \end{aligned}$$

are given in Table 3. Within the scatter of the data no temperature dependence was found for 1930 – 2455 K. The mean value of $\log (k_{8+9})$ with its error bars (double standard deviation) is

$$\log (k_{8+9}/(\mathrm{cm^3\,mol^{-1}\,s^{-1}})) = 13.89 \pm 0.26.$$

Due to the short reaction time scale a possible influence of the vibrational relaxation of hydrogen on the measured $^1CH_2$ concentration time profiles should be considered first. The mole fraction of hydrogen is sufficiently low to

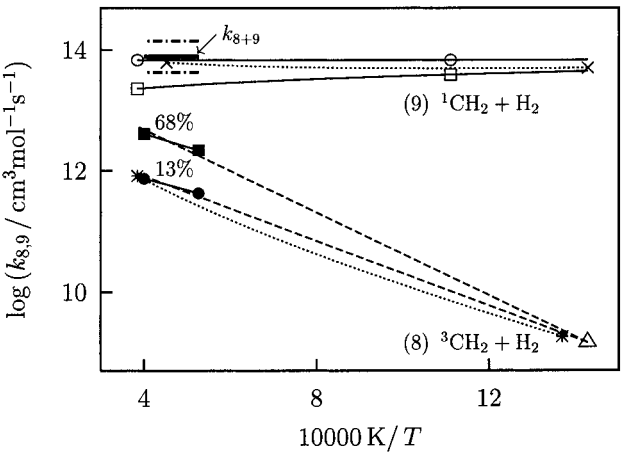

Fig. 5. Arrhenius plot of k_{8+9}. Estimation of the triplet reaction contribution by comparison with literature data. — and $-\cdot-$: k_{8+9} this work, ○: temperature independent extrapolation of $^1CH_2$ reaction, □: temperature dependent extrapolation of $^1CH_2$ reaction, ● and ■: estimation of $^3CH_2$ reaction on the basis of k_{8+9}, △: k_8 [65], - - -: interpolations of $^3CH_2$ reaction, ∗ and dotted line: estimation of $^3CH_2$ reaction given in [33], ×: k_9 calculated on the basis of the reverse reaction [66].

have no effect on the temperature behind the shock wave. On the other hand its vibrational relaxation time in argon (10 μs at 1900 K, 4 μs at 2500 K) [64] is comparable to the characteristic reaction times of 50–100 μs observed in this work. Therefore an influence of the hydrogen relaxation especially during the first few microseconds can not be ruled out. However, in thermal equilibrium, which could not be reached during these early reaction times, only 5% of the whole hydrogen is in its first vibrational excited state at 2200 K. It is very improbable that a short deviation from this low equilibrium value should have a great influence on the determined rate constant.

In Fig. 5 the obtained temperature independent rate constant is plotted in Arrhenius form and is compared to other literature data. The thick horizontal line represents the determined value of $k_{8+9} = 7.8 \cdot 10^{13}$ cm^3 mol^{-1} s^{-1} in its error bars (dash-dotted lines). Other experimental data both for the singlet and the triplet forward reactions (8) and (9) are not available for temperatures higher than 700 K. Wagener [7, 67] investigated the reaction of $^1CH_2$ with hydrogen at temperatures from 210 to 475 K by means of LIF. For the total rate constant, quenching process (k_Q, $\rightarrow$ $^3CH_2$) and reactive channel (9) (k_9, $\rightarrow$ products), he reported $k_{Q+9} = (7.3 \pm 1.0) \cdot 10^{13} \cdot (T/295\,K)^{(-0.5\pm0.6)}$ cm^3 mol^{-1} s^{-1}. The slightly inverse temperature dependence is consistent with *ab initio* calculations that predict a reaction without energy barrier [68]. The value of Wagener at room temperature ($k_{Q+9} = 8.1 \cdot 10^{13}$ cm^3 mol^{-1} s^{-1}) is in good agreement with measurements of Ashfold *et al.*

($7.8 \cdot 10^{13}$ [69]) and Langford *et al.* ($6.3 \cdot 10^{13}$ [70]). Taking into account a quenching ratio of 16% [11, 71] the value of $k_9 = 6.8 \cdot 10^{13}$ cm^3 mol^{-1} s^{-1} was used for the reactive singlet channel (9) at room temperature in this work. Starting from this value two different extrapolations were made toward high temperatures. In Fig. 5 the solid line marked with open circles represents a temperature *in*dependent extrapolation whereas the solid line marked with open squares represents a temperature dependent extrapolation based on the temperature dependence reported in [67]. In the latter case the expression $k_9 = 6.8 \cdot 10^{13} \cdot (T/295\,\mathrm{K})^{-0.5}$ cm^3 mol^{-1} s^{-1} was used, a possible additional temperature dependence of the quenching ratio [67] was not taken into account. Using the extrapolated values for k_9 at high temperatures and the value for k_{8+9} obtained in this work the rate constant of the triplet reaction (8) could be estimated applying the formula:

$$k_8 = (k_{8+9} - k_9) \cdot \frac{[^1CH_2]}{[^3CH_2]} = (k_{8+9} - k_9) \cdot \frac{1}{K(T)}. \qquad (1)$$

$K(T)$ represents the equilibrium constant of reaction (2) $^1CH_2 + M \rightleftharpoons {}^3CH_2 + M$. By this means for the rate of the triplet reaction k_8 the solid lines marked with solid circles and solid squares were obtained for the temperature *in*dependent and temperature dependent extrapolation of the singlet reaction, respectively. Thus, 13% (T-*in*dependent k_9) or 68% (T-dependent k_9) of the whole reaction proceeds via the triplet reaction. However, the exact values strongly depend on the used value for k_{8+9}.

The only measurement of reaction k_8 was performed at a temperature of 700 K and is shown in Fig. 5 by the open triangle [65]. Simple linear interpolations between this single point and the estimated k_8 values at higher temperatures (dashed lines) yield an activation energy for the triplet reaction of $E_a = 66$ or 51 kJ/mol and a preexponential factor of $1.1 \cdot 10^{14}$ or $1.0 \cdot 10^{13}$ cm^3 mol^{-1} s^{-1}, respectively. The obtained activation energies can be compared with estimations reported by Dóbé *et al.* [10] and Böhland *et al.* [12]. On the basis of a linear correlation of activation energy and dissociation energy (Evans-Polanyi) which holds for the reactions of $^3CH_2$ with several hydrocarbons both authors give an estimation for the activation energy of reaction (8). Dóbé *et al.* extrapolated $E_a \approx 49$ kJ/mol, whereas Böhland *et al.* reported $E_a \approx 42$ kJ/mol.

The dotted line in Fig. 5 refers to an estimation of the triplet reaction rate taken from GRI-Mech [33]. This estimation is based on the rate of the reaction $^3CH_2 + CH_4 \rightleftharpoons 2CH_3$ and on reactions of the isoelectronic oxygen atom. The H atom abstraction reactions of oxygen show a good correlation with homologous methylene reactions. In general, the activation energies of O(^3P) atom reactions are roughly 7 kJ/mol and the preexponentials factor are about $5-15$ times lower [12, 72].

Taking altogether, the interpolation of the triplet reaction which yields 13% triplet contribution fits better into the overall picture of $^3CH_2$ abstraction re-

actions than the interpolation yielding a 68% triplet contribution. Thus, the temperature *in*dependent interpolation of the singlet reaction (9) between room temperature and about 2200 K seems to be more probable.

Bhaskaran *et al.* [66] investigated the thermal decomposition of methane and determined the rate of the reaction $CH_3 + H \rightleftharpoons CH_2 + H_2$ by means of H-ARAS behind shock waves. The reported rate expression, $k = 1.8 \cdot 10^{14} \cdot \exp(-63\,\mathrm{kJ\,mol^{-1}}/RT)\,\mathrm{cm^3\,mol^{-1}\,s^{-1}}$, was obtained by fitting the H atom profiles using a complex reaction mechanism. The activation energy of $E_a = 63\,\mathrm{kJ/mol}$ is equal to the reaction enthalpy of the reverse reaction (-9). As the forward reaction proceeds without energy barrier and as the activation energy of the homologous triplet reaction can be estimated to be about 71 kJ/mol (reaction enthalpy 26 kJ/mol + activation energy of forward reaction $\approx 45\,\mathrm{kJ/mol}$) the expression obtained by Bhaskaran *et al.* can be assumed to describe the rate of the reverse singlet reaction (9). In Fig. 5 the dotted line marked with crosses represents the rate of the forward singlet reaction calculated via the equilibrium constant ($K(1000\,\mathrm{K}) = 538$, $K(2500\,\mathrm{K}) = 7.55$) on the basis of the expression given by Bhaskaran *et al.* The obtained curve is nearly temperature *in*dependent and the agreement with the temperature *in*dependent extrapolation of the singlet reaction at high temperatures is very good[1].

Taking altogether, the measurements and estimations both of the singlet reaction (9) and the triplet reaction (8) provide a consistent data set assuming a (nearly) temperature *in*dependent singlet reaction.

Mechanism and scaling factor

With regard to the sensitivity analysis shown for the two experiments in Fig. 2 it should be possible to reduce the complex mechanism given in Table 1 to the most important reactions (1–4) and (7). Singlet methylene profiles calculated using this reduced mechanism are also shown in the middle part of Fig. 2 as dashed lines. Whereas the initial increase and the reached maximum is still reproduced well, towards longer reaction times the agreement gets worse. The deviation is due to small but similar contributions of several other reactions which overall could not be neglegted, e.g. (6) $^3CH_2 + CH_2CO \rightleftharpoons C_2H_4 + CO$, (9) $^1CH_2 + H_2 \rightleftharpoons CH_3 + H$, (12) $CH_2 + CH \rightleftharpoons C_2H_2 + H$ and (15) $^3CH_2 + CH_3 \rightleftharpoons C_2H_4 + H$.

The scaling factors ζ, which convert the measured FM signal level to $^1CH_2$ concentration, are shown as function of temperature in Fig. 6. It was shown

[1] Baulch *et al.* [40] calculated the rate of the reverse reaction (-9) on the basis of a temperature independent value of $k_9 = 7.2 \cdot 10^{13}\,\mathrm{cm^3\,mol^{-1}\,s^{-1}}$ and obtained a value for k_{-9} which is 6 times lower than the corresponding value of Bhaskaran *et al.* In contrast to that in this work forward and reverse reaction are consistent. This discrepancy is probably due to a typing error in the reported expression for the equilibrium constant in [40].

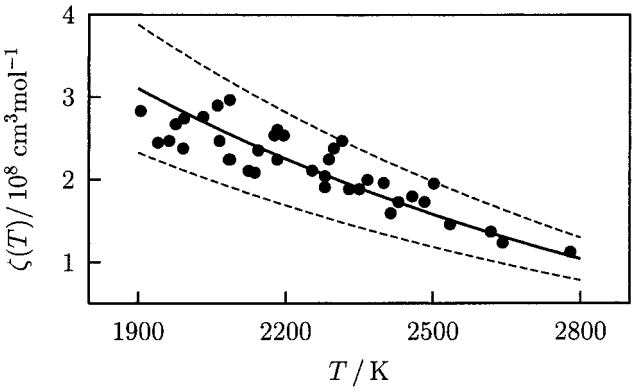

Fig. 6. Calibration function obtained for $^1CH_2$. Experimental conditions: modulation index = 1.45, modulation frequency = 965 MHz, experimental pressure = 640 mbar (T = 1500 K) to 320 mbar (T = 3100 K). — Fit, - - - Fit ±25%.

in [18] that the following simple relation holds for FM measurements:

$$I_{\mathrm{FM}}^{\max} = I_o \cdot c \cdot \zeta.$$

$I_{\mathrm{FM}}^{\max}$ refers to the measured FM signal intensity, I_o is the total intensity of the laser beam, c is the species concentration and ζ refers to the calibration function. ζ describes the temperature (and pressure) dependence of the scaling factor and varies with modulation frequency (here 965 MHz) and modulation index (here 1.45). Thus, ζ comprises the temperature and pressure dependence of the absorption coefficient, the temperature and pressure dependence of the FM factor (which takes into account some extra lineshape effects relevant for FM spectroscopy) and an apparatus constant of the used FM spectrometer. It is possible to convert the calibration function to the absorption coefficient and, vice versa, to calculate the calibration function on the basis of a known absorption coefficient. For further details see [18].

In Fig. 6 the obtained calibration function ζ (solid line) is shown with its 25% error bars (dashed lines). If the calibration function should be used to determine the absorption coefficient of $^1CH_2$ an additional influence of the reaction mechanism should be taken into account. Due to fast consecutive reactions the CH_2 concentration does not reach a maximum value of $[CH_2]_{\mathrm{tot}}^{\max} = [CH_2CO]_o$. For example, at a temperature of 2500 K and at 500 mbar total pressure only 31% of an initial ketene mole fraction of 1000 ppm could be detected as CH_2. It can be seen from Fig. 1 that a variation of the rate constants of the most sensitive reactions (1) and (3) by a factor of two results in a change of the simulated maximum $^1CH_2$ concentration (and with it the scaling factor and the calibration function) of approximately 30%.

5. Conclusions

The formation of CH_2 during the thermal decomposition of ketene has been investigated at temperatures from 1905 to 2780 K and pressures around 450 mbar and could be described by a complex reaction mechanism. For the unimolecular decomposition reaction, (1) $CH_2CO + M \rightarrow CH_2 + CO + M$, the rate constants obtained in that range of pressure and temperature are

$$k_1 = (9.5 \pm 5.7) \cdot 10^{15} \cdot \exp\left[(-244 \pm 25)\,\mathrm{kJ\,mol^{-1}}/RT\right] \mathrm{cm^3\,mol^{-1}\,s^{-1}}.$$

For the reaction (3a) and (3b), $CH_2 + CH_2 \rightarrow C_2H_2 + 2\,H$ and $\rightarrow C_2H_2 + H_2$ a channel distribution of 50% and a rate expression of

$$k_{3a} = k_{3b} = 3.8 \cdot 10^{14} \cdot \exp\left(-29.5\,\mathrm{kJ\,mol^{-1}}/RT\right) \mathrm{cm^3\,mol^{-1}\,s^{-1}}$$

allows a consistent description of the experimental data.

The high temperature methylene reaction $(8+9)$ $^{1,3}CH_2 + H_2 \rightarrow CH_3 + H$ was investigated at temperatures from 1930 to 2455 K at pressures around 500 mbar. For the total rate constant a temperature independent value was obtained:

$$\log\left(k_{8+9}/(\mathrm{cm^3\,mol^{-1}\,s^{-1}})\right) = 13.89 \pm 0.26.$$

On the basis of low temperature literature data and the systematics of activation energies of triplet methylene reactions the rate constants of the singlet and triplet reactions could be estimated to be

$$k_9 = 6.8 \cdot 10^{13}\ \mathrm{cm^3\,mol^{-1}\,s^{-1}}$$
$$k_8 = 1.0 \cdot 10^{13} \cdot \exp\left(-51\,\mathrm{kJ\,mol^{-1}}/RT\right) \mathrm{cm^3\,mol^{-1}\,s^{-1}}.$$

This corresponds to a triplet reaction contribution of 13% at 2200 K.

The quantitative detection of $^1CH_2$ as described in this paper allows the determination of the absorption coefficient of $^1CH_2$ at high temperatures. The conversion procedure of the calibration function to the absorption coefficient is described in [18].

Quantitative detection of $^1CH_2$ enables further direct investigations of methylene reactions at high temperatures and could serve as a verification of complex hydrocarbon combustion mechanisms which were developed in recent years. Measurements of $^1CH_2$ profiles during the thermal decomposition of methane and ethane behind shock waves have already been performed [73].

Acknowledgement

The active help of J. Deppe and the support by DFG and Fonds der Chemie are gratefully acknowledged.

References

1. J. Warnatz, *18th Symp. (Int.) on Combust.*, The Combustion Institute, Pittsburgh (1981), p. 369.
2. Ch. Dombrowsky and H. Gg. Wagner, Ber. Bunsenges. Phys. Chem. **96** (1992) 1048, p. 373.
3. C. P. Fenimore, *13th Symp. (Int.) on Combust.*, The Combustion Institute, Pittsburgh (1971).
4. J. A. Miller and C. F. Melius, Combust. Flame **91** (1992) 21.
5. P. Jensen and P. R. Bunker, J. Chem. Phys. **89** (1988) 1327.
6. P. P. Gaspar and G. S. Hammond, R. A. Moss and M. Jones (eds.), *Carbenes*, vol. 2, New York (1975), p. 207.
7. M. Koch, F. Temps, R. Wagener and H. Gg. Wagner, Z. Naturforsch. **44a** (1989) 195.
8. W. Hack, M. Koch, R. Wagener and H. Gg. Wagner, Ber. Bunsenges. Phys. Chem. **93** (1989) 165.
9. H.-H. Carstensen and H. Gg. Wagner, Ber. Bunsenges. Phys. Chem. **99** (1995) 1539.
10. S. Dóbé, T. Böhland, F. Temps and H. Gg. Wagner, Ber. Bunsenges. Phys. Chem. **89** (1985) 432.
11. T. Böhland, F. Temps and H. Gg. Wagner, Ber. Bunsenges. Phys. Chem. **89** (1985) 1013.
12. T. Böhland, S. Dóbé, F. Temps and H. Gg. Wagner, Ber. Bunsenges. Phys. Chem. **89** (1985) 1110.
13. U. Bley, F. Temps, H. Gg. Wagner and M. Wolf, Ber. Bunsenges. Phys. Chem. **96** (1992) 1043.
14. A. D. Sappey, D. R. Crosley and R. A. Copeland, Appl. Phys. B **50** (1990) 463.
15. V. A. Lozovsky, I. Derzy and S. Cheskis, *27th Symp. (Int.) on Combust.*, The Combustion Institute, Pittsburgh (1998), p. 445.
16. A. McIlroy, Chem. Phys. Lett. **296** (1998) 151.
17. J. Deppe, G. Friedrichs, H.-J. Römming, A. Ibrahim and H. Gg. Wagner, Ber. Bunsenges. Phys. Chem. **102** (1998) 1474.
18. G. Friedrichs and H. Gg. Wagner, Z. Phys. Chem. **214** (2000), 1723.
19. K. Holzrichter and H. Gg. Wagner, *18th Symp. (Int.) on Combust.*, The Combustion Institute, Pittsburgh (1981), p. 769.
20. G. Friedrichs, *Frequenzmodulierte Spektroskopie zur Untersuchung von Reaktionen des Amino- und Methylenradikals hinter Stoßwellen*, Cuvillier-Verlag, Göttingen (1999), ISBN 3-89712-741-5, Ph.D. thesis, Universität Göttingen.
21. R. J. Kee, F. M. Ruply and J. A. Miller, *Chemkin-II: A Fortran Chemical Kinetics Package for the Analysis of Gas-Phase Chemical Kinetics*, Sandia Report SAND89-8009, Sandia National Laboratories, Livermore, California (1989), http://www.ca.sandia.gov/chemkin/.
22. A. A. Konnov, *Detailed reaction mechanism for small hydrocarbons combustion. Release 0.3* (1997), http://homepages.vub.ac.be/∼akonnov/.1997.
23. H. Carstensen, *Untersuchungen von Elementarreaktionen des Singulett-Methylens* $CH_2(\tilde{a}^1A_1)$ *mit Hilfe der Laser-Induzierten-Fluoreszenz*, Ph.D. thesis, Universität Göttingen (1995), MPI für Strömungsforschung Bericht 4/1995.
24. G. Friedrichs and H. Gg. Wagner, Z. Phys. Chem. **203** (1998) 1.
25. M. W. Markus, P. Roth and A. M. Tereza, *25th Symp. (Int.) on Combust.*, The Combustion Institute, Pittsburgh (1994), p. 705.
26. P. Frank, K. A. Bhaskaran and T. Just, J. Phys. Chem. **90** (1986) 2226.
27. S. Bauerle, M. Klatt and H. Gg. Wagner, Ber. Bunsenges. Phys. Chem. **99** (1995) 870.

28. P. R. Bunker, P. Jensen, W. P. Kraemer and R. Beardsworth, J. Chem. Phys. **85** (1986) 3724.
29. A. R. W. McKellar, P. R. Bunker, T. J. Sears, K. M. Evenson, R. J. Saykally and S. R. Langhoff, J. Chem. Phys. **79** (1983) 5251.
30. D. G. Leopold, K. K. Murray, A. E. S. Miller and W. C. Lineberger, J. Chem. Phys. **83** (1985) 4849.
31. M. Litorja and B. Ruscic, J. Chem. Phys. **108** (1998) 6748.
32. I.-C. Chen, W. H. Green, Jr. and C. B. Moore, J. Chem. Phys. **89** (1988) 314.
33. G. P. Smith, D. M. Golden, M. Frenklach, N. W. Moriarty, B. Eiteneer, M. Goldenberg, C. T. Bowman, R. Hanson, S. Song, W. C. Gardiner Jr., V. Lissianski and Z. Qin, *GRI-Mech Version 3.0* (1999), http://www.me.berkeley.edu/gri_mech.
34. P. Frank and T. Just, Symp. Int. Shock Tubes Proc. **14** (1984) 706.
35. Ch. Dombrowsky, Universität Göttingen, unpublished results.
36. D. Fulle and H. Hippler, J. Chem. Phys. **106** (1997) 8691.
37. W. Boullart and J. Peeters, J. Phys. Chem. **96** (1992) 9810.
38. H. Okabe, *Photochemistry of Small Molecules*, John Wiley & Sons, New York (1978).
39. T. Böhland, F. Temps and H. Gg. Wagner, J. Phys. Chem. **91** (1987) 1205.
40. D. L. Baulch, C. J. Cobos, R. A. Cox, C. Esser, P. Frank, T. Just, J. A. Kerr, M. J. Pilling, J. Troe, R. W. Walker and J. Warnatz, J. Phys. Chem. Ref. Data **21** (1992) 411.
41. T. Böhland, F. Temps and H. Gg. Wagner, Ber. Bunsenges. Phys. Chem. **90** (1986) 468.
42. W. Tsang and R. F. Hampson, J. Phys. Chem. Ref. Data **15** (1986) 1087.
43. J. A. Miller and C. T. Bowman, Prog. Energy Combust. Sci. **15** (1989) 287.
44. M. Bartels, J. Edelbüttel-Einhaus and K. Hoyermann, *23th Symp. (Int.) on Combust.*, The Combustion Institute, Pittsburgh (1991), p. 131.
45. A. A. Konnov, *Detailed reaction mechanism for small hydrocarbons combustion. Release 0.4* (1998), http://homepages.vub.ac.be/∼akonnov.
46. D. L. Baulch, C. J. Cobos, R. A. Cox, P. Frank, G. Hayman, T. Just, J. A. Kerr, T. Murrells, M. J. Pilling, J. Troe, R. W. Walker and J. Warnatz, Combust. Flame **98** (1994) 59.
47. A. J. Dean and R. K. Hanson, J. Quant. Spectrosc. Radiat. Transfer **42** (1989) 375.
48. K. H. Homann and C. Wellmann, Ber. Bunsenges. Phys. Chem. **87** (1983) 609.
49. M. Röhrig, E. L. Petersen, D. F. Davidson, R. K. Hanson and C. T. Bowman, Int. J. Chem. Kin. **29** (1997) 781.
50. A. J. Dean and R. K. Hanson, Int. J. Chem. Kinet. **24** (1992) 517.
51. R. Möller, E. Mozzhukhin and H. Gg. Wagner, Ber. Bunsenges. Phys. Chem. **90** (1986) 854.
52. P. Roth, U. Barner and R. Löhr, Ber. Bunsenges. Phys. Chem. **83** (1979) 929.
53. M. W. Markus, P. Roth and T. Just, Int. J. Chem. Kinet. **28** (1996) 171.
54. R. Hartig, J. Troe and H. Gg. Wagner, *13th Symp. (Int.) on Combust.*, The Combustion Institute, Pittsburgh (1971), p. 147.
55. T. Kruse, *Untersuchungen zu Hochtemperaturreaktionen von Kohlenwasserstoffradikalen mit atom- und molekülspektroskopischen Methoden*, Ph.D. thesis, Universität - Gesamthochschule - Duisburg (1999).
56. J. Warnatz, W. C. Gardiner Jr. (ed.), *Combustion Chemistry*, chap. 5, Springer Verlag, New York (1985).
57. J. H. Kiefer and S. S. Kumaran, J. Phys. Chem. **97** (1993) 414.
58. W. Tsang, J. Phys. Chem. Ref. Data **20** (1991) 221.
59. P. Frank, K. A. Bhaskaran and T. Just, *21th Symp. (Int.) on Combust.*, The Combustion Institute, Pittsburgh (1986), p. 885.
60. N. Cohen and K. R. Westberg, J. Phys. Chem. Ref. Data **12** (1983) 531.
61. H. Gg. Wagner and F. Zabel, Ber. Bunsenges. Phys. Chem. **75** (1971) 114.

62. S. K. Kim, E. R. Lovejoy and C. B. Moore, J. Chem. Phys. **102** (1995) 3202.
63. R. A. King, W. D. Allen, B. Ma and H. F. Schaefer III, Faraday Discuss. **110** (1998) 23.
64. J. E. Dove and H. Teitelbaum, Chem. Phys. **6** (1974) 431.
65. H. Gg. Wagner, unpublished results.
66. K. A. Bhaskaran, P. Frank and T. Just, A. Lifshitz and J. Rom (eds.), *Proc. 12th Int. Symp. Shock Tubes and Waves*, The Magnes Press, The Hebrew University of Jerusalem (1980), p. 503.
67. R. Wagener, *Untersuchung von Reaktionen der Singulett-Carbene* $CH_2(\tilde{a}^1A_1)$ *und* $CHCl(\tilde{X}^1A')$ *in der Gasphase*, Ph.D. thesis, Universität Göttingen (1990), MPI für Strömungsforschung Bericht 4/1990.
68. C. Sosa and H. B. Schlegel, J. Am. Chem. Soc. **106** (1984) 5847.
69. M. N. R. Ashfold, M. A. Fullstone, G. Hancock and G. W. Ketley, Chem. Phys. **55** (1981) 245.
70. A. O. Langford, H. Petek and C. B. Moore, J. Chem. Phys. **78** (1983) 6650.
71. B. Himme, *Reaktionen von Sauerstoffatomen und Methylenradikalen mit ungesättigten Kohlenwasserstoffen. Erprobung der Hg-Sensibilisierten* N_2O *Photolyse bei hohen Drucken*, Ph.D. thesis, Universität Göttingen (1977).
72. R. E. Huie and J. T. Herron, Prog. Reaction Kinetics **8** (1975) 1.
73. J. Deppe, *Reaktionskinetik kleiner Moleküle hinter Stoßwellen unter Verwendung empfindlicher spektroskopischer Methoden*, Cuvillier Verlag, Göttingen (2000), ISBN 3-89712-986-8, Ph.D. thesis, Universität Göttingen.